Physica Scripta. Vol. T76, 93–97, 1998

Intermode Traces – Fundamental Interference Phenomenon in Quantum and Wave Physics

A. E. Kaplan,[1,2] P. Stifter,[1] K. A. H. van Leeuwen,[3] W. E. Lamb, Jr.[4] and W. P. Schleich[1]

[1] Abteilung für Quantenphysik, Universität Ulm, 89069 Ulm, Germany*
[2] Permanent address: Electr. & Comp. Eng. Dept., The Johns Hopkins University, MD 21210, USA
[3] Physics Dept., Eindhoven University of Technology, 5600 MB Eindhoven, The Netherlands
[4] Optical Sciences Center, University of Arizona, AZ 85721, USA

Received October 21, 1997; accepted January 8, 1998

PACS Ref: 03.65.Bz

Abstract

Highly regular spatio-temporal or multi-dimensional patterns in the quantum mechanical probability or classical field intensity distributions can appear due to pair interference between individual eigen-modes of the system forming the so called intermode traces. These patterns are strongly pronounced if the intermode traces are multi-degenerate. This phenomenon occurs in many areas of wave physics.

1. Introduction

A fundamental feature of wave physics, in particular quantum mechanics and electrodynamics, is the phenomenon of interference. Its most striking manifestation is Young's double slit experiment [1]. In this article we focus on and explain a new class of interference effects: the formation of highly regular spatio-temporal or multidimensional patterns in the quantum mechanical probability, $|\psi|^2$, or classical field intensity, $|\mathcal{E}|^2$, distributions. We show that the underlying building blocks of these patterns are the intermode traces which arise from the pair interference between individual eigen-modes of the system; the phenomenon is strongly pronounced for highly degenerate traces. These traces appear in such diverse systems as a confined quantum particle, atoms scattered at a periodic laser-induced grating, an electromagnetic (EM) waveguide, and light diffraction. In Fig. 1 we show this phenomenon for the example of a quantum particle trapped in a box with infinitely steep and high walls; we note characteristic zig-zag canals and ridges in space-time. A similar picture emerges in an EM waveguide with metallic walls. Moreover, the straight canal patterns in the intensity of light scattered by the diffraction grating, as well as in the quantum probability of almost resonant atoms scattered by a periodic standing laser wave, as shown in Fig. 2, are multi-replicas of the single box zig-zag patterns. Curved canals and ridges exist for the case of a quantum particle confined to a smooth potential forming the "quantum carpet" depicted in Fig. 3.

The first indications of canals in a quantum box emerged from computer simulations [2] of the motion of a Gaussian wave packet and from the analysis [3] of the dynamics of an initially homogeneous wave function. Similar patterns also arise in the near field of a diffraction grating [4]. The canals in the quantum box for initially well localized wave packets, were explored [5] either using the wave functions directly [5], or the Wigner phase space distributions [6]. Another approach [7] averages the probability along the canals. So far all the treatments of these structures have relied on the specific choice of the initial wave function and the potential. However, this obscures the mechanism of the pattern formation. In this article we identify pair interference between the

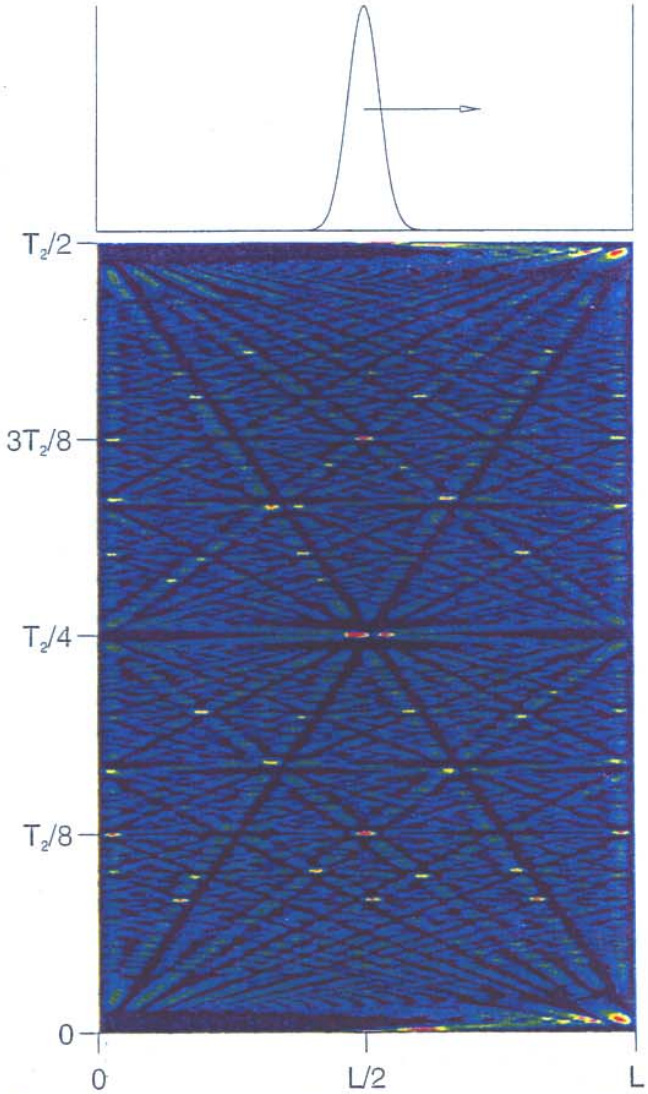

Fig. 1. An initial wavefunction with a single peak (top) creates canals and ridges (bottom) in space-time (x, t); these patterns are formed by highly degenerate intermode traces in a density distribution of $|\psi|^2$ in a box potential.

* e-mail: schleich@physik.uni-ulm.de

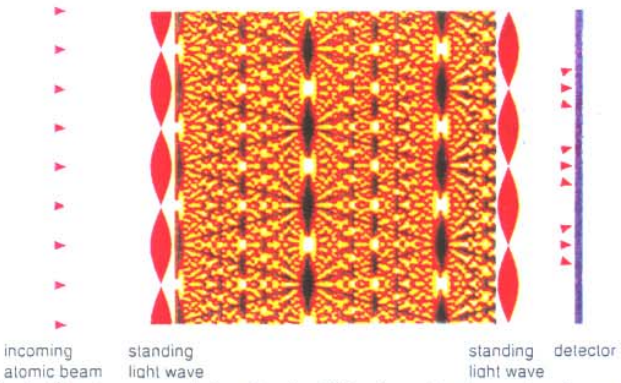

Fig. 2. Quantum carpet in atomic diffraction. A plane atomic wave (collimated atomic beam) of metastable krypton atoms is incident from the left. The atomic wave interacts with a standing light wave, whose nodes act as holes of a spatially-periodic transmission grating for metastable atoms. Zero to maximum probability density is shown on a color-coded scale from black via red, orange and yellow through white.

eigenmodes of the system and the degeneracy of this interference as the key mechanisms for this phenomenon. Thus, the quantum carpet is woven by the thread of intermode traces, each of which is formed by just two individual eigenmodes.

The wave function $\psi(r, t)$ of a quantum particle with mass m_e moving in a potential $U(r)$ is governed by the Schrödinger equation,

$$i\hbar \frac{\partial \psi}{\partial t} - [\hat{T} + U(r)]\psi = 0. \tag{1}$$

Here $\hbar$ is the Planck constant, and $\hat{T} \equiv -(\hbar^2/2m_e)\nabla^2$ is the operator of kinetic energy. Maxwell's equations of classical electrodynamics can also be approximated by the same equation under the assumption of small diffraction and fixed polarization. In a resulting scalar equation, ψ is replaced by the field amplitude $\mathscr{E}$, U by the dielectric constant ε, ∇^2 by the "transverse" Laplacian, time t by the longitudinal coordinate z of propagation, and $\hbar$ by the wavelength λ. The limits $\hbar \to 0$ and $\lambda \to 0$ correspond to classical mechanics and ray optics, respectively. This so-called paraxial approximation is valid for many problems related to the optics of well collimated fields, e.g. in lasers and some microwave devices. In this article we consider for simplicity only one-dimensional problems, or precisely speaking, problems which involve either spatio-temporal wave patterns in quantum mechanics with one coordinate and a time variable, or spatial patterns in optics with one transverse and one longitudinal variable.

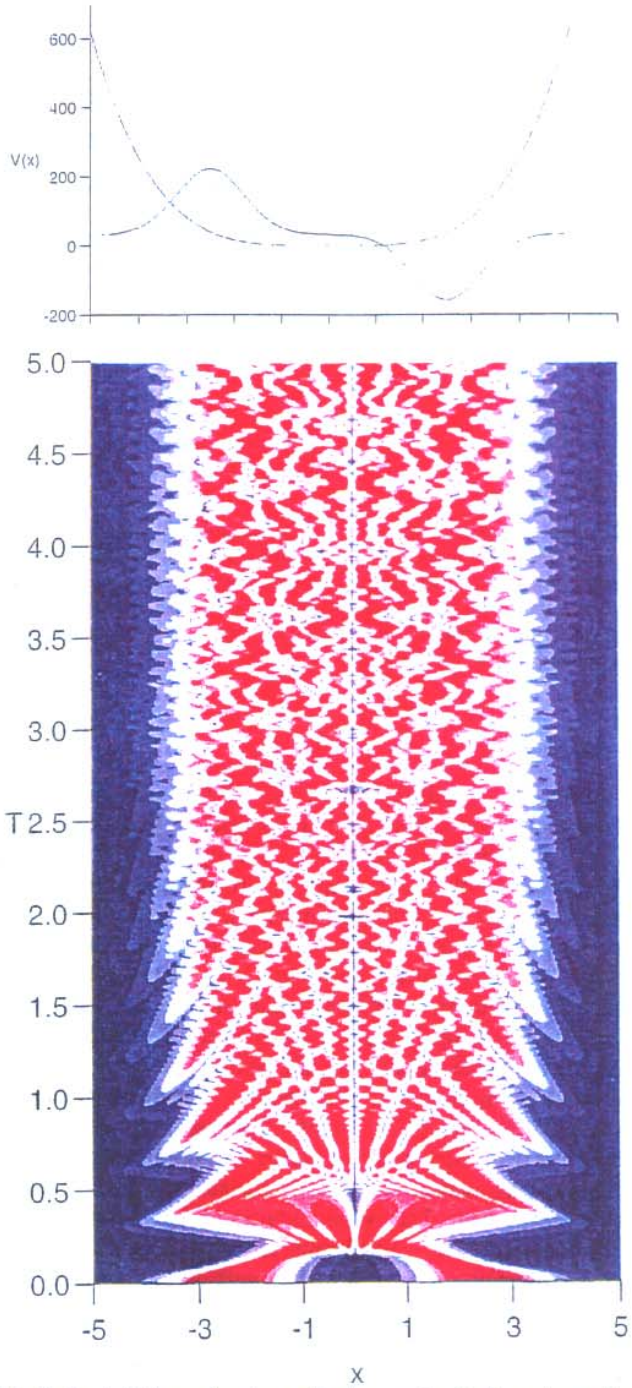

Fig. 3. An initial wavefunction with two peaks (top) creates patterns (bottom) in a density distribution of $|\psi|^2$ in space-time (x, t), with spatially resolved groups of individual intermode traces, in a smooth yet sufficiently "hard" potential well $U(x) \propto x^4$.

2. Particle in the box

We first consider the problem of an electron in a quantum box with infinite walls. In the electrodynamic analog, this corresponds to an EM wave in a waveguide with ideal metallic walls. The box problem was at the center of a discussion [8] between Max Born and Albert Einstein on the propagation of a quantum wave packet in a box as opposed to the classical bouncing of the particle. In that discussion, Max Born focused on the notion of a classical particle as a packet of many quantum eigenmodes and considered the earlier stages of the diffusion of the packet. However, he did not proceed far enough to observe the phenomenon of revivals of the package, nor the ordered quantum patterns discussed here.

For a box of size L along the x axis where $\nabla^2 = \partial^2/\partial x^2$, we introduce the ground-state frequency, $\omega_1 = \hbar\pi^2/(2m_e L^2)$, and wavenumber, $k_1 = \pi/L$, in terms of which the eigen-frequencies, eigen-energies and eigen-wavenumbers are $\omega_n = n^2\omega_1$, $E_n = \hbar\omega_n$ and $k_n = nk_1$, respectively, with $n = 1, 2, 3, \ldots$. The normalized eigen-wavefunctions are then $\psi_n(x, t) = \sqrt{2/L} \sin(k_n x) \exp(-i\omega_n t)$ and vanish at $x = 0$ and L. The full wavefunction is $\psi = \sum_{n=1}^{\infty} a_n \psi_n(x, t)$, where the eigen-amplitudes a_n are determined by the initial conditions.

To bring out the spatio-temporal patterns of the probability distribution, $|\psi(x,t)|^2 = \sum_{n=1}^{\infty}\sum_{m=1}^{\infty}\mu_{nm}$, we represent the intermode term,

$$\mu_{nm} \equiv \frac{1}{2}\, a_n a_m^* \psi_n \psi_m^* + c.c.$$

$$= \frac{1}{L}\, a_n a_m^* \sin(k_n x)\sin(k_m x)\, e^{i(\omega_m-\omega_n)t} + c.c. \qquad (2)$$

as a sum of four elementary "interference waves",

$$\mu_{nm} = \frac{|a_n a_m|}{2L}\{\cos[(k_n - k_m)x + (\omega_n - \omega_m)t - \phi_{nm}]$$
$$+ \cos[(k_n - k_m)x - (\omega_n - \omega_m)t + \phi_{nm}]$$
$$- \cos[(k_n + k_m)x + (\omega_n - \omega_m)t - \phi_{nm}]$$
$$- \cos[(k_n + k_m)x - (\omega_n - \omega_m)t + \phi_{nm}]\}. \qquad (3)$$

Hence the lines of constant phases $(k_n \pm k_m)x \pm (\omega_n - \omega_m)t = const.$ define "traces" in space-time; in the present box problem they are straight lines. According to (3), the amplitude product $a_n a_m^*$ determines the "weight" of the (n, m)-trace via $|a_n a_m|$, and its positioning via the phase ϕ_{nm}, defined by $\exp(i\phi_{nm}) = a_n a_m^*/|a_n a_m|$. The main players in trace formation, however, are the "velocities" of the traces:

$$v_{nm} \equiv \left(\frac{dx}{dt}\right)_{nm} = \pm\frac{\omega_n - \omega_m}{k_n \pm k_m},$$

or

$$v_{nm} = \pm(n \pm m)\cdot qc. \qquad (4)$$

Here c is the velocity of light, and $q = \lambda_C/4L \ll 1$ is a small parameter with $\lambda_C = 2\pi\hbar/cm_e = 2.4\times10^{-10}$ cm, being the Compton wavelength. We note that $dx/dt \propto N$, with N – integer, and hence, all the traces with a number N are attributed to all the couples of modes that satisfy the condition $|n \pm m| = N$. This trace degeneracy creates multiple superimposed traces with the same N. They in turn give rise to the distinct canals seen in Fig. 1 on a fluctuating background.

This degeneracy can be lifted by any factor disturbing the ideal box model. For the sake of illustration we consider here relativistic corrections, which provide the most fundamental perturbation, although in realistic settings they are very small [9]. Assuming with great margin that $E_n \ll m_e c^2$ and using the Schrödinger eq. (1) with the corrected kinetic energy operator, $\hat{T} \approx -(\hbar^2\nabla^2/2m_e)\cdot(1 + \hbar^2\nabla^2/4m_e^2c^2)$, we obtain the relativistically shifted eigen-energies, $E_n = n^2(1 - q^2n^2)\hbar\omega_1$. The trace velocities (4) are then modified, which lifts the degeneracy:

$$\frac{dx}{dt} = \pm(n \pm m)[1 - q^2(n^2 + m^2)]qc. \qquad (5)$$

The maximal relative correction is $\Delta_{max} \sim -E_{max}/4m_e c^2$, where E_{max} is the maximum possible energy of an electron in a system; e.g. for 2 eV-deep quantum well, $|\Delta_{max}| \sim 10^{-6}$.

3. General binding potential

The box potential makes it relatively easy to illustrate and explain the intermode traces. However, the phenomenon is not restricted to the box; it occurs for many potentials. To generalize our results, we note that the first of the eq. (4) holds true regardless of the potential. Indeed, (4) can be obtained by: (*i*) recalling that the intermode terms $\mu_{nm} \equiv (1/2)(a_n a_m^* \psi_n \psi_m^* + c.c.)$ are combinations of the functions $f_n f_m \exp\{i\int[\pm k_n(x) \pm k_m(x)]\,dx - i(E_n - E_m)t/\hbar\}$; (*ii*) by analyzing their lines of constant phase in the same way as for the box problem; and (*iii*) by keeping in mind that for sufficiently large excitation, the amplitude envelopes $f_n(x)$ vary slowly compared to $\exp[i\int k_n(x)\,dx]$. Note that now k_n is position-dependent. For highly excited states it is well approximated by the WKB method [10] as $k_n(x) = \hbar^{-1}\sqrt{2m_e[E_n - U(x)]}$. Hence, in WKB the trace velocities for an arbitrary potential are

$$v_{nm}(x) \equiv \left(\frac{dx}{dt}\right)_{nm} \approx \pm\frac{\omega_n - \omega_m}{k_n(x) \pm k_m(x)}$$
$$= \pm\frac{(E_n - E_m)/\sqrt{2m_e}}{\sqrt{E_n - U(x)} \pm \sqrt{E_m - U(x)}}. \qquad (6)$$

The trace trajectory is then $t = \int_{x_1}^{x} v_{nm}^{-1}\,dx$, where x_1 is one of the turning points determined by $E_n = U(x)$. The eigen-energy E_n is evaluated within WKB from $\int_{x_1}^{x_2} k_n\,dx = \pi(n + 1/2)$, where x_2 is the other turning point. For $U \propto |x|^w$ with $w > -2$, we [11] find $E_n \propto n^{2w/(2+w)}$.

An initially almost classical motion is described by a compact group of eigen-modes near some high quantum number N, with a total number ΔN of these modes satisfying the condition $1 \ll \Delta N \ll N$. This excitation results in a strong clustering of the traces in two groups. The one with $|k_n \pm k_m| \ll |k_N|$, is essentially a classical trajectory, since in such a case $(\omega_n - \omega_m)/(k_n \pm k_m) \approx d\omega/dk \equiv v_{gr}$, where v_{gr} is a group velocity. But $v_{gr}(E_N)$ coincides with the classical velocity, since the trace equation obtained from (6) as $dx/dt = \sqrt{2[E_N - U(x)]/m_e}$, describes the classical motion of a particle with the energy E_N in a potential $U(x)$. Thus, this group of traces is a quantum entity reproducing the classical trajectory in the limit $\hbar \to 0$ even when the Ehrenfest theorem is inadequate. Indeed, it was shown [12] that for a box, the direct ensemble averaging of quantum trajectories $\langle x(t)\rangle$ *does not* reproduce the classical trajectory as $\hbar \to 0$. The other group of traces, with $dx/dt \ll v_{gr}$, corresponds to $|k_n \pm k_m| \approx |2k_N|$, and reflects the quantum behavior related to the revival phenomenon [12, 13].

To excite many eigen-modes using a ground state as an initial wavefunction, one needs to shake-up the system by a strong EM pulse shorter than the cycles of excited eigen-frequencies. The potential avenues to realize these pulses either via cascade stimulated Raman scattering or unipolar, subfemtosecond solitons ("EM-bubbles") were recently outlined in Refs. [14] and [15, 16], respectively.

Distinct patterns near the classical trajectory are better pronounced for strongly anharmonic potentials with "hard walls", the extreme example of which is a box. They are less pronounced for "soft" potentials, e.g. $U \propto |x|^w$ with $w \leqslant 2$, including a harmonic potential, $w = 2$. This is explained by a strong degeneracy in a box, whereby many individual traces with the *same* velocity bundle together to form the patterns. The soft potentials, on the other hand, originate non-degenerate traces. To illustrate this, we note from (6) that the peak velocity, i.e. at $U(x) = 0$, of a near-classical trace, is $(v_{nm})_{pk} \approx \pm(\sqrt{E_n} + \sqrt{E_m})/\sqrt{2m_e}$. Hence, if $E_n \propto n^2$, as in a box, then according to eq. (4) $(v_{nm})_{pk} \propto n + m$, and

there are many couples n and m producing the same v_{pk}. However, for a harmonic potential, where $E_n \propto n$, the only quantum numbers resulting in *exact* degeneracy of $(v_{nm})_{pk}$, are $n, m = 1, 4, 9, 16$, etc.; thus there are very few degenerate traces.

Looking now into the set of position-dependent $v_{nm}(x)$, where n, m are *near* some fixed integer $N \gg 1$, with $n \equiv N + \Delta n$ and $m \equiv N + \Delta m$, $|\Delta n \pm \Delta m| \ll N$, for the potential $U \propto |x|^w$, we have

$$v_{nm}(x) \approx v_{gr}(E_N, x)\left[1 + \frac{\Delta n + \Delta m}{N}\left(\frac{w/2}{2+w}\right) \times \left(\frac{E_N}{E_N - U(x)}\right) - \frac{\Delta n^2 + \Delta m^2}{N^2}\left(\frac{w/4}{(2+w)^2}\right) \times \left(\frac{E_N}{E_N - U(x)}\right)\left(2 + \frac{wU(x)}{E_N - U(x)}\right) + \cdots\right]. \quad (7)$$

Without the term with $\Delta n^2 + \Delta m^2$, all the traces with e.g. $\Delta n + \Delta m = 0$ would be degenerate. Comparing this term with the previous one at $|\Delta n + \Delta m| = 1$, we find the number of eigenmodes $\Delta N_d \equiv |\Delta n - \Delta m|_{max}$, forming one group of nearly-degenerate traces, as

$$\Delta N_d \sim \sqrt{N}\sqrt{\frac{2+w}{2 + wU(x)/(E_N - U(x))}}.$$

Near the point $U(x) = 0$, the ratio $\Delta N_d/\sqrt{N}$ increases as w increases; for a box, $w = \infty$. We note also that this ratio decreases in the area $E_N/2 < U(x) < E_N$ (which is very narrow for hard potentials), especially as we approach a turning point, $U(x) \to E_N$. The space-time locations of tight bunching of the nearly-degenerate traces, $x_{mn}(t)$, depend on the specific initial conditions. For example, if the initial wavefunction is a fast moving tight packet near a turning point, where it hits the hard wall, it should make a tight bunch of traces at that point, after which the traces will fan out as they approach the opposite wall, and after reflection from that wall, come close together again as they return back to the first wall. This behavior is clearly seen in Fig. 3 that depicts well pronounced patterns for a smooth, yet still sufficiently hard potential $U \propto x^4$.

4. Diffraction intermode carpets in optics

The intermode traces are readily found in optics and electrodynamics, with waveguides, resonators and spatially- or time-periodical structures providing a natural background for EM mode interference. Maxwell's equations which even in their scalar form differ from the Schrödinger eq. (1), can be reduced to it in the case of small diffraction within the paraxial approximation (PA). The scalar PA equation in free space, $2ik\partial\mathscr{E}/\partial z + \partial^2\mathscr{E}/\partial x^2 = 0$, for the field envelope $\mathscr{E}$ propagating along the z axis and having cross-section coordinate x, is isomorphous to (1) with $U \equiv 0$. Thus, for example, the modes of a sufficiently wide, $L \gg \lambda$, waveguide with ideally conducting walls will have the same patterns as those of a quantum box, with the intermode traces in the distribution of $|\mathscr{E}|^2$ having "tilts" similar to the velocities (4).

Even more interesting as far as optical applications, e.g. spectroscopic devices, are concerned, would be the traces in the field scattered by a diffraction grating. To reproduce the "box" modes, one can use two plane waves, symmetrically incident upon the grating under the angle of incidence θ, provided we choose θ such that $2L \sin\theta = \lambda(1 + 2n)$, $n = 0, 1, 2, \ldots$; the smallest θ in PA is $\theta \approx \lambda/2L$. Due to this configuration, the fields at any two adjacent slits of the grating will have the same amplitudes but opposite phases. If the maximum of the full field is positioned at one of the slits, the field in the middle between the slits *beyond* the grating, will exactly vanish, thus making multi-replicas of the waveguide with metallic walls or quantum box with infinitely-high walls.

5. Quantum carpets in atom optics

A quantum carpet of a similar multi-box structure can be observed not only with light and electrons, but also with atoms. An initial "plane atomic wave" is formed then by a well-collimated beam of atoms in a long-lived metastable state. An effective diffraction grating can be produced by letting these atoms interact with a standing light wave. The light is tuned to an atomic transition from the metastable state to an upper state, which preferentially decays to the ground state. Hence, after passing the standing light wave most atoms will be optically pumped into the ground state. However, atoms passing close to the nodes of the standing wave, where no light is present, will still remain in the metastable state, and can be selectively detected. Thus, for these atoms, the laser light acts as a transmission grating with narrow slits. The resulting diffraction pattern is shown in Fig. 2, which depicts the probability density of the atoms in the metastable state on a color-coded scale. A plane atomic wave of metastable atoms is incident from the left, where the atoms intersect the standing laser wave, which is vertical in the figure. We note that the density drops to almost zero (black) except near the nodes; further to the right, the characteristic canal patterns develop. They can be observed now using a second standing light wave and a surface ionization detector which measures the total intensity of the metastable atoms transmitted through both light fields. The second light wave can again be considered as a narrow-slit grating. This grating probes the probability distribution pattern: the transmitted intensity is large only if the slits coincide with local maxima in the pattern. This detection scheme is depicted on the right of Fig. 2. By varying the horizontal distance between the light fields, as well as the phase offset in the vertical direction, the "carpet" can be accurately reconstructed from the detector signal. The demands on an actual experiment are stringent. The beam has to be collimated to an angular spread below 0.1 mrad in order to develop a coherent, plane atomic wave and the axial velocity of the atoms has to be equal to within a few percent. These demands can be met by using laser-cooling techniques to prepare the beam. We plan to perform such an experiment using a 100 m/s axial velocity beam of metastable krypton atoms, with the two diffracting light beams of $\lambda = 769$ nm. Reference [17] reports the first experimental indications of such a quantum carpet for atoms.

6. Extensions and related phenomena

The intermode trace phenomenon can be extended to other areas of wave physics. Its existence does not depend on the

exact form or order of the wave equations; the linearity however, is required since it allows for eigen-modes. One can relate well known wave phenomena such as the so called Kikuchi lines in X-ray diffraction in crystals [18], Chladni patterns in acoustics, and the formation of straight patches of calm surface in rough seas, to the intermode traces. They are also reminiscent of scars [19] in quantum billiards and may therefore provide new insights into these fingerprints of quantum chaos. In more general terms, even many nonlinear wave equations, such as the nonlinear Schrödinger, Kordeweg-De Vries, and sine-Gordon equations, are able to support multi-soliton solutions with the individual solitons having their trajectories reminiscent of intermode traces. Straight multi-soliton traces have recently been found [16] in a modified Kordeweg-De Vries equation approximating the propagation of EM-bubbles [15, 16]. Much more complicated yet highly organized two-dimensional nonlinear-optical patterns are formed both in the near-field and far-field areas by the grid of spatial dark solitons [20], and in a resonator filled with a Kerr-like nonlinear material [21]. All these wave phenomena might have the same roots as the quantum traces discussed here. They pave the way to the physics of well-organized "carpet" macro-structures in multi-wave systems with a broad-spectrum excitation.

Acknowledgements

We thank P. Bardroff, M. V. Berry, I. Bialynicki-Birula, M. Fontenelle, O. Friesch, F. Grossmann, N. Imoto, C. Leichtle, J. Marklof, I. Marzoli, M. M. Nieto, J.-M. Rost, F. Saif, E. Wolf and A. Zeilinger for many fruitful and enlightening discussions. One of us (WPS) expresses his sincere thanks to the organizing committee of this Nobel Symposium and especially to Prof. E. Karlsson for organizing a most splendid and interesting meeting. AEK and WEL gratefully acknowledge the support of the Alexander von Humboldt Foundation. The work of WPS is supported by the Deutsche Forschungsgemeinschaft.

References

1. Young, T., Phil. Trans. Royal Soc. 12 (1802), also 387 (1802) and 1 (1804).
2. Kinzel, W., Phys. Bl. **51**, 1190 (1995).
3. Berry, M. V., J. Phys. **A29**, 6617 (1996).
4. Berry, M. V. and Klein, S., J. Mod. Opt. **43**, 2139 (1996).
5. Grossmann, F., Rost, J. M. and Schleich, W. P., J. Phys. **A30**, L277 (1997).
6. Stifter, P., Leichtle, C., Schleich, W. P. and Marklof, J., Z. Naturforsch. **52a**, 377 (1997).
7. Marklof, J., "Limit theorems for theta sums with applications in quantum mechanics" (Shaker Verlag, Aachen 1997).
8. Einstein, A., "Scientific papers presented to M. Born" (Oliver and Boyd, London 1953), pp. 33; Born, M., Kgl. danske Vidensk. Selsk. mat-fys. Medd. **30**, 2 (1955); Born, M. and Ludwig, W., Z. Phys. **150**, 106 (1958).
9. Relativistic-like corrections resulting from a higher order paraxial approximation in optics were studied in Ref. [4].
10. See, e.g. Bohm, D., "Quantum theory" (Prentice-Hall, Englewood Cliffs, New York 1951).
11. Nieto, M. M. and Simmons Jr., L. M., Am. J. Phys. **47**, 643 (1979).
12. Ballentine, L. E., Yang, Y. and Zibin, J. P., Phys. Rev. **A50**, 2854 (1994).
13. Leichtle, C., Averbukh, I. Sh. and Schleich, W. P., Phys. Rev. Lett. **77**, 3999 (1996).
14. Kaplan, A. E., Phys. Rev. Lett. **73**, 1243 (1994).
15. Kaplan, A. E. and Shkolnikov, P. L., Phys. Rev. Lett. **75**, 2316 (1995).
16. Kaplan, A. E., Straub, S. F. and Shkolnikov, P. L., Opt. Lett., **22**, 405 (1997); also J. Opt. Soc. Am. **B14**, 3013 (1997).
17. Nowak, S., Kurtsiefer, Ch., Pfau, T. and David, C., Opt. Lett. **22**, 1430 (1997).
18. Kikuchi, S., Jap. J. Phys. **5**, 83 (1928).
19. Heller, E., Phys. Rev. Lett. **53**, 1515 (1984); Wilkinson, P. B., *et al.* Letter to Nature **380**, 606 (1996).
20. Swartzlander, G. A., Andersen, D. R., Regan, J. J., Yin, H. and Kaplan, A. E., Phys. Rev. Lett. **66**, 1583 (1991).
21. Akhmanov, S. A., Vorontsov, M. A. and Ivanov, V. Yu., J. Exp. Theor. Phys. Lett. **47**, 707 (1988); Firth, W. J., J. Mod. Opt. **37**, 151 (1990); D'Alessandro, G. and Firth, W. J., Phys. Rev. Lett. **66**, 2597 (1991); Arecchi, F. T., Giacomelli, G., Ramazza, P. L. and Residori, S., Phys. Rev. Lett. **65**, 2531 (1990); Residori, S., Ramazza, P. L., Pampaloni, E., Boccaletti, S. and Arecchi, F. T., Phys. Rev. Lett. **76**, 1063 (1996).